Inorganic Chemistry

Article

pubs.acs.org/IC

Cadmium(II) Complex Formation with Selenourea and Thiourea in Solution: An XAS and ^{113}Cd NMR Study

Farideh Jalilehvand,* Zahra Amini, and Karnjit Parmar

Department of Chemistry, University of Calgary, Calgary, AB, Canada T2N 1N4

Supporting Information

ABSTRACT: The complexes formed in methanol solutions of $Cd(CF_3SO_3)_2$ with selenourea (SeU) or thiourea (TU), for thiourea also in aqueous solution, were studied by combining ^{113}Cd NMR and X-ray absorption spectroscopy. At low temperature (~200 K), distinct ^{113}Cd NMR signals were observed, corresponding to CdL_n^{2+} species (n = 0–4, L = TU or SeU) in slow ligand exchange. Peak integrals were used to obtain the speciation in the methanol solutions, allowing stability constants to be estimated. For cadmium(II) complexes with thione (C═S) or selone (C═Se) groups coordinated in $Cd(S/Se)O_5$ or $Cd(S/Se)_2O_4$ (O from MeOH or $CF_3SO_3^-$) environments, the ^{113}Cd chemical shifts were quite similar, within 93–97 ppm and 189–193 ppm, respectively. However, the difference in the chemical shift for the $Cd(SeU)_4^{2+}$ (578 pm) and $Cd(TU)_4^{2+}$ (526 ppm) species, with $CdSe_4$ and CdS_4 coordination, respectively, shows less chemical shielding for the coordinated Se atoms than for S, in contrast to the common trend with increasing shielding in the following order: O > N > Se > S. In solutions dominated by mono- and tetra-thiourea/selenourea complexes, their coordination and bond distances could be evaluated by Cd K-edge extended X-ray absorption fine structure (EXAFS) spectroscopy. At ~200 K and high excess of thiourea, a minor amount (up to ~30%) of $[Cd(TU)_{5-6}]^{2+}$ species was detected by an upfield shift of the ^{113}Cd NMR signal (up to 423 ppm) and an amplitude reduction of the EXAFS oscillation. The amount was estimated by fitting linear combinations of simulated EXAFS spectra for $[Cd(TU)_4]^{2+}$ and $[Cd(TU)_6]^{2+}$ complexes. At room temperature, $[Cd(TU)_4]^{2+}$ was the highest complex formed, also in aqueous solution. Cd L_3-edge X-ray absorption near edge structure (XANES) spectra of cadmium(II) thiourea solutions in methanol were used to follow changes in the CdS_xO_y coordination. The correlations found from the current and previous studies between ^{113}Cd NMR chemical shifts and different Cd(II) coordination environments are generally useful for evaluating cadmium coordination to thione-containing or Se-donor ligands in biochemical systems or for monitoring speciation in solution.

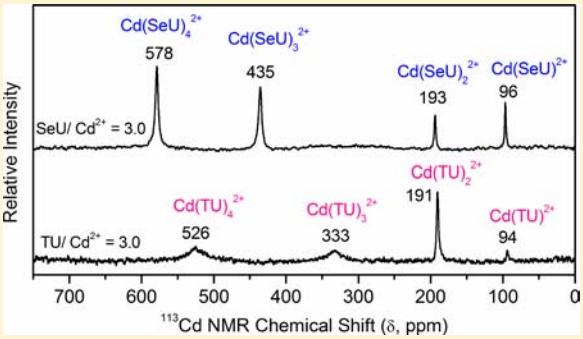

INTRODUCTION

Thione-containing molecules have important biochemical functions and also industrial applications. For example, L-ergothioneine (a thiohistidine) is a naturally occurring amino acid with antioxidant properties that can be made by few organisms (bacteria and fungi), taken up by plants and ingested by animals and human.[1] It has two tautomeric forms: thiol and thione;[2] the latter predominates at physiological pH in aqueous solution,[3] and can form complexes with many metal ions: Cu(II) > Hg(II) > Zn(II) > Cd(II) > Ni(II) ~ Co(II), in order of increasing stability.[4,5] Some diabetic patients obtain high levels of ergothioneine, which, due to the high stability of its zinc complexes (log $\beta_2 \sim 10^{12}$),[4] leads to zinc deficiency and glucose intolerance.[6] Also, it has been shown that ergothioneine has protective effects toward cadmium-induced teratogenesis.[7]

Increasing our knowledge about how interactions related to group 12 zinc(II) and cadmium(II) ions affect biological systems is essential. Although its ionic radius is larger (~0.2 Å),[8] cadmium(II) is known to attach to the binding sites of Zn-enzymes/proteins with higher affinity than zinc(II) and thereby inhibit important functions.[9,10] Thiourea (TU, Scheme 1) provides a structurally simple model for studies of thione-containing ligands. The structures of many metal–thiourea complexes, in which the thiourea molecule is coordinated to the metal center via its S atom, are available in the Cambridge structural database (CSD),[11] such as the four-coordinated $[Cd(TU)_2Cl_2]$[12] and $[Cd(TU)_4](NO_3)_2$,[13] and the six-coordinated $[Cd(TU)_2(NO_3)_2]$,[13] $[Cd(TU)_2(HCOO)_2]$,[14]

Scheme 1. Thiourea (TU) and Selenourea (SeU)

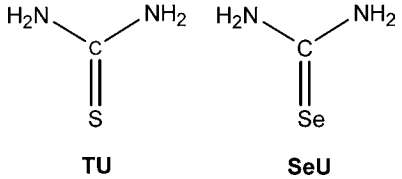

Received: April 26, 2012
Published: September 27, 2012

and $[Cd(TU)_6](ReO_4)_2$ complexes.[15] In aqueous solution, cadmium(II) complexes with up to four thiourea ligands have been reported with the formation constants $\beta_1 = 20$, $\beta_2 = 140$, $\beta_3 = 260$, and $\beta_4 = 1200$ (Figure S-1 of the Supporting Information), based on a polarographic study.[16]

CdS semiconducting nanoparticles (NPs) and thin films have promising photoelectrochemical applications, for example, in solar cells.[17] Highly luminescent water-soluble CdS NPs can be prepared by thermal decomposition of Cd(II) and thiourea mixtures. Their size influences the optical activity,[18] and the photoluminescence quantum yield depends on pH and on the concentration and ratio of thiourea to cadmium(II).[19,20] O'Brien and Saeed deposited thin films of CdS from alkaline solutions of $Cd(CH_3COO)_2$, ethylenediamine, and thiourea, and they correlated the quality and morphology of CdS thin films to the conditions used for growth, for example, by following speciation changes in the solution by ^{113}Cd NMR spectroscopy.[21] The observed ^{113}Cd NMR chemical shifts, however, were not connected to specific Cd(II) species. ^{113}Cd NMR spectroscopy has also been used to investigate the formation mechanism of Cd NPs through oxidative aggregation of $[Cd_{10}S_4Br_4(SR)_{12}]^{4-}$ (SR = *p*-tolylthiolate) by elemental sulfur.[22]

CdSe NPs and thin films have been prepared from mixtures of selenourea and cadmium salts in similar ways as for cadmium sulfide. Selenourea (SeU, Scheme 1) is a resonance-stabilized selenoketone (selone) with π-conjugation between the selenocarbonyl and amino groups.[23] It is sensitive to heat, light, and moisture and is easily oxidized in acidic aqueous solution, forming a Se−Se bond in a diselenobis-(formamidinium) cation,[24] or decomposed by atmospheric oxygen to red elemental selenium in neutral/alkaline aqueous solution,[25] and even in methanol and ethanol.[26] Hydrolytic decomposition of selenourea generates cyanamide (H_2CN_2), Se^{2-}, and HSe^-, and is accelerated by increasing pH.[25,27,28] Hydrochemical decomposition of metal selenourea compounds to metal selenide nanoparticles is a common procedure for generating thin films for new semiconductor materials.[27]

While several reports on the syntheses of simple selenourea metal complexes all conclude that the Se atom is the only coordination site for metal ions,[26,29,31] very few crystal structures are available[32,33] (apart from a few with selenourea derivatives). There is only one structurally known complex where a selenourea derivative, *N*,*N*′-diphenylselenourea, acts as a bidentate ligand with (Se, N) coordination to a Pt(II) ion.[34] A series of selenourea complexes with different Co(II), Zn(II), Cd(II), and Hg(II) salts, including $Cd(SeU)_2X_2$ (X = halide), were prepared and carefully analyzed using electronic (UV−vis) and vibrational (IR) spectroscopic techniques, reporting metal−selenium stretching vibrations within the range 167−245 cm^{-1}.[35] A solid state ^{113}Cd NMR spectrum of $[Cd(SeU)_2Cl_2]$ showed an isotropic chemical shift of $\delta_{iso}(^{113}Cd)$ = 458 ppm.[36] Recently, spray hydrolysis of $[Cd(SeU)_2Cl_2]$ in aqueous solution, prepared by reacting $CdCl_2$ hydrate with 4-fold selenourea, was used to generate CdSe films.[37] CdSe nanocrystals have also been prepared by fast injection of a base to a solution of $Cd(NO_3)_2{\cdot}4H_2O$ and selenourea at room temperature. The mechanism of this reaction seems to be via an unidentified intermediate Cd−selenourea complex.[38] A polarographic study showed that Cd(II) ions form a selenourea complex with limited solubility in deaerated water with $[Cd^{2+}]$ = 0.01 mM.[39] The formation constant for the 1:1 complex between cadmium(II) and SeU was recently determined to be $\log \beta_1 = 2.11 \pm 0.04$ in 0.5 mol dm^{-3} $HClO_4$ and ionic strength I = 1.0 ($NaClO_4$) at 298 K using UV−vis spectroscopy,[40] which differs from the previously reported value $\log \beta_1 = 0.9$ ($\log \beta_2$ = 3.7) using a cadmium amalgam electrode.[41]

In the current study, we compared the complex formation of cadmium(II) ions with selenourea and thiourea as ligands, keeping $C_{Cd(II)}$ = 0.1 mol dm^{-3} and varying the mole ratios SeU/Cd(II) from 1.0 to 5.0 and TU/Cd(II) from 1.0 to 20.0. The speciation and structure of the complexes were investigated with ^{113}Cd NMR spectroscopy as the main tool, complemented by Cd K-edge EXAFS and Cd L_3-edge XANES spectra. Methanol was chosen as solvent because selenourea reacts with water,[25] and it also allowed low temperature studies (at ∼200 K). In addition, the cadmium(II)−thiourea complexes formed in aqueous solution were studied at room temperature.

^{113}Cd NMR spectroscopy has in the past few decades developed into a powerful tool for studying the coordination of cadmium ions in compounds and biological systems.[42,43] The ^{113}Cd NMR chemical shift depends on several factors, including the following: number and type of the donor atoms (with the general trend O > N > Se > S, in order of increasing shielding) and the coordination geometry around cadmium, the nature and charge of the ligand (e.g., different shielding of sulfur in thiolate S^- and thiocyanate SCN^-), and its coordination mode (bridging vs terminal).[43,44] This is evident from the ^{113}Cd NMR isotropic chemical shifts (δ_{iso}) for crystalline Cd(II) complexes with *S*-thione containing ligands in Table 1 and from the ^{113}Cd NMR chemical shifts for Cd(II) complexes with Se-donor ligands in Table 2. In solution, ligand-exchange dynamics affects the peak shape and peak position, which becomes a weighted average of the chemical shifts of all Cd(II) species involved in fast ligand-exchange equilibria.[45] The temperature and the nature of the solvent also influence the ^{113}Cd NMR chemical shift.

Table 1. Solid State ^{113}Cd NMR Isotropic Chemical Shifts (δ_{iso}) for Crystalline Cd(II) Complexes with *S*-Thione Containing Ligands[a]

Cd(II)-thione compds[b]	coordination	^{113}Cd NMR chem shift (δ_{iso}, ppm)	ref
$[Cd(tztH)_4](CF_3SO_3)_2$	CdS_4	605[c]	46
$[Cd(TU)_4](NO_3)_2$	CdS_4	577 (this work)	13
$[Cd(TU)_2Cl_2]$	CdS_2Cl_2	462[d]	36
$[Cd(tzt)_2]$	CdS_2N_2	430[c]	47
$[Cd(DMTF)_6](ClO_4)_2$	CdS_6	402 (this work)	48
$(HIm)[Cd(tsac)_3(H_2O)]$	CdS_3O	378 (this work)	49
$[Cd(TU)_3(SO_4)]$	CdS_3O	346 (this work)	50
$[Cd_2(6\text{-}MP)_4(H_2O)_2](NO_3)_4$	CdS_3N_2O	313	51
trans-$[Cd(DMTF)_4(CF_3SO_3)_2]$	CdS_4O_2	263 (this work)	48
$[Cd_2(6\text{-}MP)_4(NO_3)_2](NO_3)_2$	$CdS_3N_2O_2$	233	51
cis-$[Cd(TU)_2(H_2O)_4](SO_4)$	CdS_2O_4	148 (this work)	52

[a]See Figures S-3 and S-4(a, b). [b]tztH = 1,3-thiazolidine-2-thione, DMTF = dimethylthioformamide, HIm = imidazolium, tsac = thiosaccharinato (with negatively charged thionate-*S*),[49] 6-MP = 6-mercaptopurine. [c]The calibration is shifted (see the text) by changing δ_{iso} for the solid reference compound $3CdSO_4{\cdot}8H_2O$ from −77.4 to −58 ppm. [d]The calibration is shifted by changing δ_{iso} for the solid reference compound $Cd(NO_3)_2{\cdot}4H_2O$ from −132.2 to −100 ppm.

dx.doi.org/10.1021/ic300852t | *Inorg. Chem.* 2012, 51, 10619−10630

Table 2. ^{113}Cd NMR Chemical Shifts for Mononuclear Cd(II) Complexes with Se-Donor Ligands

Cd(II) compds[a]	coordination	^{113}Cd NMR chem shift (δ, ppm)	ref
$[Cd(dmpSe)_2](ClO_4)_2$	$CdSe_2P_2$	670 (CH_2Cl_2, 193 K)	55
$Cd[N(^iPr_2PSe)_2]_2$	$CdSe_4$	629 (solid)	56
CdSe (bulk)	$CdSe_4$	558 (solid)[b]	57, 58
$[Cd(SePh)_4](NO_3)_2$	$CdSe_4$	533 (CH_3OH, 213 K)[c]	59
$Cd(L\text{-ImSe})_2Cl_2$	$CdSe_2Cl_2$	506–591 (solid)[d]	60
$Cd(SeU)_2Cl_2$	$CdSe_2Cl_2$	490 (solid)[d]	36
$[Cd(Se\text{-aryl})_2(bpy)]$	$CdSe_2N_2$	460, 472 (solid), 411 ($CHCl_3$)	61
$[Cd(SeC(O)R')_2(tmeda)]$	$CdSe_2N_2O_2$	388–391 ($CDCl_3$)[e]	62
$[Cd(SeC_5H_4N)_2(tmeda)]$	$CdSe_2N_4$	300 ($CDCl_3$)[e]	63
$(Ph_4P)[Cd(SeC(O)Tol)_3]$	$CdSe_3O_2$	250 (CH_2Cl_2, 193 K)	64

[a]dmpSe = $Ph_2PCH_2P(Se)Ph_2$; $N(^iPr_2PSe)_2^-$ = tetraisopropyldiselenoimidodiphosphoinato; $^-$SePh = phenylselenolate; L-ImSe = imidazolidine-2-selone, L = H, CH_3, C_2H_5, n-C_3H_7, i-C_3H_7; Se-aryl = $^-$Se-2,4,6-$^iPr_3$-C_6H_2; R′ = Ph, Tol, Tol = C_6H_4-p-CH_3; tmeda = *N*,*N*,*N*′,*N*′-tetramethylethylenediamine. [b]The value reported here is referenced relative to $Cd(ClO_4)_2$ (aq) by changing the chemical shift of solid $Cd(NO_3)_2{\cdot}4H_2O$ from 0.0 to −100 ppm.[43] [c]The calibration for 4.5 mol·dm^{-3} $Cd(NO_3)_2$ (aq) was changed from −65 to −73 ppm. [d]The calibration was adjusted by changing δ_{iso} for $Cd(NO_3)_2{\cdot}4H_2O$ from −132.2 to −100 ppm. [e]Reported relative to $Cd(CH_3COO)_2{\cdot}2H_2O$ in CH_3OD (0.0 ppm).

^{113}Cd NMR chemical shifts from different sources are sometimes calibrated with different standards.[53] To keep consistency in Tables 1 and 2 between our ^{113}Cd chemical shifts calibrated as 0 ppm for solid $Cd(ClO_4)_2{\cdot}6H_2O$ and those previously reported, we have used −100 ppm as calibration point for solid $Cd(NO_3)_2{\cdot}4H_2O$, and −45 and −58 ppm for the two signals for solid $3CdSO_4{\cdot}8H_2O$.[54] For the solution spectra, our calibration 0 ppm for 0.1 mol·dm^{-3} $Cd(ClO_4)_2$ (aq) corresponds to −73 ppm for 4.5 mol·dm^{-3} $Cd(NO_3)_2$(aq) (Table 2).[43]

The low temperature measurements presented here show that at ∼200 K the Cd(II)−selenourea and most Cd(II)−thiourea complexes are in slow ligand-exchange, resulting in a separate ^{113}Cd NMR peak for each Cd(II) complex (Figure 1). Their peak positions and areas allowed quantitative speciation of the Cd(II)−thione/selone complexes and also an estimate of their stability constants. The EXAFS studies of the solutions with a dominating Cd(II)−thione/selone complex corroborated the assignments of the ^{113}Cd NMR resonances and provided additional structural information.

The results and the methodology used in this research provide benchmarks for evaluating coordination environments involving Cd(II) ions and thione/selone groups in complex biological systems or for monitoring speciation in solution, e.g. to control the formation of CdS/CdSe nanoparticles via thiourea/selenourea complexes.

EXPERIMENTAL SECTION

Sample Preparation. Selenourea, thiourea, and methanol-d_4 (CD_3OD) from Sigma-Aldrich were used without further purification. Methanol (MeOH) was dried by refluxing twice over magnesium

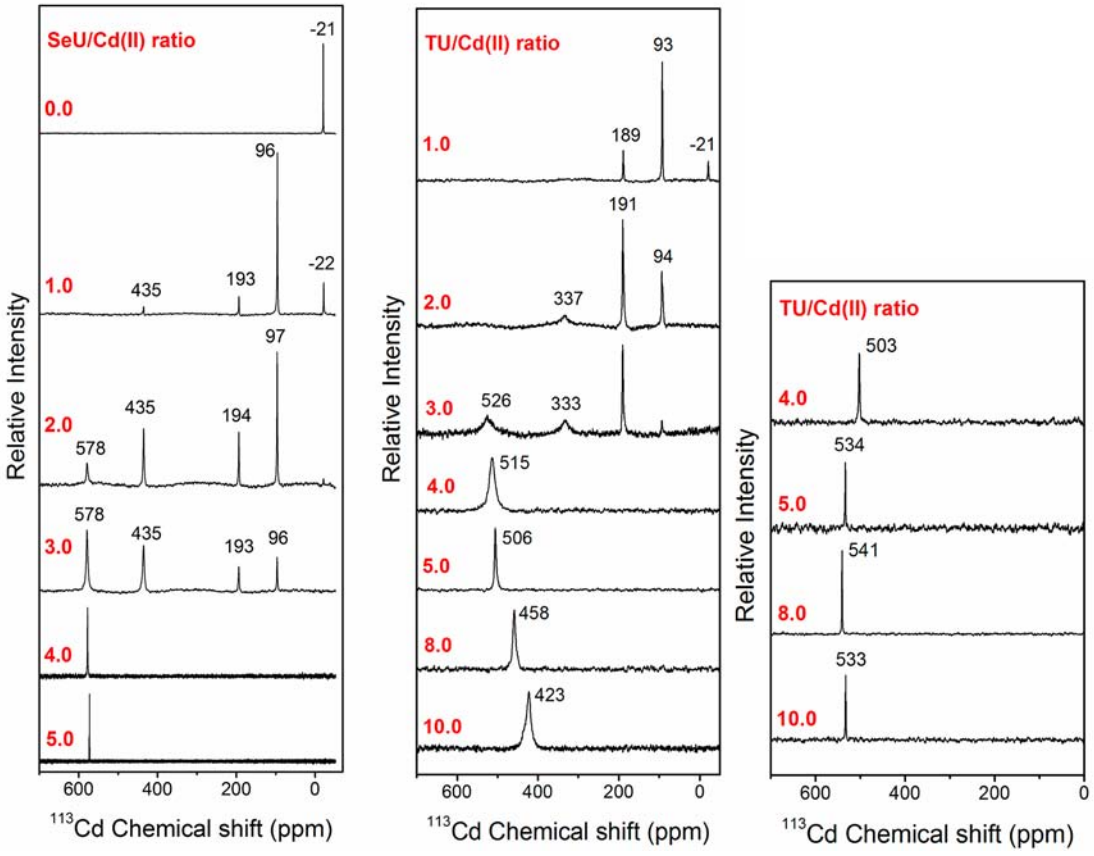

Figure 1. ^{113}Cd NMR spectra of 0.1 mol dm^{-3} $Cd(CF_3SO_3)_2$ methanol solutions with increasing mole ratios L/Cd(II) of selenourea (**S1**−**S5**; *left*, at 203 K) or thiourea (**T1**−**T7**; *middle* at 203 K; *right* at 295 K). For notations see Table 3.

dx.doi.org/10.1021/ic300852t | *Inorg. Chem.* 2012, 51, 10619−10630

turnings under argon atmosphere. Dehydrated cadmium triflate $Cd(CF_3SO_3)_2$ was prepared by dissolving freshly prepared $Cd(OH)_2$ in triflic acid, in a procedure described previously.[65]

Cadmium(II) Selenourea/Thiourea Solutions. Cadmium(II) triflate solutions with $[Cd^{2+}]_{tot}$ = 0.1 mol dm^{-3} and varying amounts of SeU or TU in O_2-free, dried methanol were prepared in a glovebox with dry inert atmosphere. For the ^{113}Cd NMR measurements, the solvent contained 30% CD_3OD. Five solutions with SeU/Cd(II) mole ratios of 1.0 (**S1**), 2.0 (**S2**), 3.0 (**S3**), 4.0 (**S4**), and 5.0 (**S5**) were prepared. Higher SeU/Cd(II) mole ratios were prevented by the limited solubility of SeU in methanol at ∼200 K. Similar cadmium(II) thiourea solutions in methanol were prepared with the TU/Cd(II) mole ratios 1.0 (**T1**), 2.0 (**T2**), 3.0 (**T3**), 4.0 (**T4**), 5.0 (**T5**), 8.0 (**T6**), and 10.0 (**T7**). To check the solvent effect, a parallel series of Cd(II)-thiourea solutions (**W1** to **W9**) were prepared in distilled water containing 10% D_2O. Table 3 presents the composition of the solutions.

Table 3. Composition of the Cadmium(II)−Selenourea and Thiourea Solutions[a]

soltns in MeOH	L/Cd^{II} mol ratio	$[Cd^{2+}]_{total}$ (mmol·dm^{-3})	$[L]_{total}$ (mmol·dm^{-3})	soltns in H_2O
		L = SeU		
S1	1.0	100	100	
S2	2.0	100	200	
S3	3.0	100	300	
S4	4.0	100	400	
S5	5.0	100	500	
		L = TU		
T1	1.0	100	100	**W1**
T2	2.0	100	200	**W2**
T3	3.0	100	300	**W3**
T4	4.0	100	400	**W4**
T5	5.0	100	500	**W5**
T6	8.0	100	800	**W6**
T7	10.0	100	1000	**W7**
		100	1500	**W8**
		100	2000	**W9**

[a]For ^{113}Cd NMR measurements, the methanol solutions contained 30% CD_3OD and aqueous solutions 10% D_2O.

^{113}Cd NMR Reference Compounds. The crystalline cadmium(II) dimethylthioformamide (DMTF) compounds $[Cd(DMTF)_6](ClO_4)_2$ (coordination model for CdS_6) and $[Cd(DMTF)_4(CF_3SO_3)_2]$ (CdS_4O_2 model), imidazolium tris(thiosaccharinato)aquacadmate(II) $(HIm)[Cd(tsac)_3(H_2O)]$ (CdS_3O model), and $[Cd(TU)_4](NO_3)_2$ (CdS_4 model) were synthesized according to descriptions in the literature,[13,48,49] and they were verified by comparing their unit cell dimensions with those of the known structures (Figure S-2 of the Supporting Information).

^{113}Cd NMR Measurements. The ^{113}Cd NMR spectra of the methanol solutions **S1**−**S5** and **T1**−**T7** were collected at 203 K with a Bruker DRX-400 spectrometer at 88.56 MHz, using a 5 mm broadband (BBO) probe, a zgdc pulse program, a sweep width of 800 ppm, and a recycle delay of 3.0 s. All the above solutions contained ∼30% CD_3OD. A 0.1 mol·dm^{-3} solution of $Cd(ClO_4)_2·6H_2O$ in D_2O was used as external reference (0 ppm at 295 K).[43] The temperature of the instrument was calibrated using ^{1}H NMR of methanol.[66] The spectra of the Cd(II)-thiourea solutions **T1**−**T7** in methanol and **W1**−**W9** in water (10% D_2O) were also measured under similar conditions at room temperature (295 K). The total number of scans collected for each sample can be found in Table S-1a. The integrated areas of the peaks in the ^{113}Cd NMR spectra of the methanol solutions **T1**−**T3** and **S1**−**S3** (203 K) are listed in Table S-1b.

Solid state ^{113}Cd NMR spectra of the crystalline cadmium(II) reference compounds were measured using a Bruker AMX 300 spectrometer equipped with a MAS BL4 double-resonance broadband probe, at the resonance frequency 66.59 MHz. The samples were packed into 4 mm ZrO rotors with magic angle spinning (MAS) rates between 5 and 8 kHz. Solid $Cd(ClO_4)_2·6H_2O$ was used for calibration (0 ppm at room temperature). Spectra were acquired at 300 K using a 4 μs ^{1}H 90° pulse, a 4 ms contact time, and a 10 s recycle delay. The isotropic chemical shifts are listed in Table 1.

X-ray Absorption Spectroscopy. Cadmium K-edge EXAFS spectra of the solutions **S1**, **S5**, and **T1**−**T7** were collected at BL 7-3, and Cd L_3-edge XANES spectra of solutions **T1**−**T7** were measured at room temperature at BL 4−3 at the Stanford synchrotron radiation lightsource (SSRL) with the storage ring operated at 3.0 GeV and 150−200 mA. The EXAFS spectra for solutions **S1** and **S5** were measured at 200 K (LT) by means of a liquid-helium cryostat, while for **T1**−**T7** spectra were collected both at 200 K and at room temperature (RT). Pure methanol solidifies below ∼179 K, so by keeping the temperature at 200 K the samples remained unfrozen and were kept inside the cryostat under chilled air flow (not vacuum) at all times (*Note:* N_2 in the air freezes below ∼80 K). At BL 7-3, higher harmonics from the Si(220) double crystal monochromator were rejected by detuning to 50% of the maximum incident beam (I_0) intensity, while a Rh-coated mirror was used at BL 4-3 to eliminate higher harmonics from a fully tuned Si(111) double crystal monochromator. The EXAFS spectra were recorded in transmission mode, with all ion chambers filled with argon, while the Cd L_3-edge XANES spectra were measured in fluorescence mode using a PIPS solid state detector (I_f) and a helium-filled ion chamber (I_0) monitoring the X-ray fluorescence and incident beam intensities, respectively. For EXAFS measurements, the samples were held between Kapton windows in 2 mm pinhole cells sealed with vacuum grease at LT, or in 5 mm Teflon spacers at RT. Two to six scans (10 for **S1**) were collected for each sample. During the Cd L_3-edge XANES measurements, two scans were measured for each solution held within a 5 mm Teflon spacer between 4 μm Ultralene windows that were found to resist penetration of He gas that otherwise could form bubbles in the sample. Before averaging the overlapping scans using the EXAFSPAK program,[67] the energy scale was externally calibrated for each scan by assigning the first inflection point of the Cd K- and L_3-edge of a Cd foil to 26711.0 and 3537.6 eV, respectively.

XAS Data Analysis. The WinXAS 3.1 program suite was used for the data analysis.[68] The background absorption was subtracted with a first-order polynomial over the pre-edge region, followed by normalization of the edge step. For the Cd K-edge EXAFS spectra, the energy scale was converted into k-space, where $k = [(8\pi^2 m_e/h^2)(E - E_0)]^{1/2}$, using the threshold energy E_0 = 26709.7−26711.0 (**S1**, **S5**) or 26710.0−26713.0 eV (**T1**−**T7** and **W1**−**W7**). The EXAFS oscillation was then extracted using a 7-segment cubic spline to remove the atomic background absorption above the edge. Details on extraction of structural parameters from the experimental EXAFS oscillation can be found elsewhere.[69] Theoretical EXAFS oscillations, $\chi(k)$, were constructed using the FEFF 8.1 program,[70,71] with FEFF input files generated by means of the ATOMS program[72] using the crystal structures of $Cd(SCH_2CH_2NH_2)_2$,[73] $[Cd(dmise)_4][PF_6]_2$, where *dmise* = 1,3-dimethyl-2(3H)-imidazoleselone,[74] and $[Cd(CH_2(COO)_2)(TU)_2]$[75] (replacing S by Se in the input file), with CdS_3N_2, $CdSe_4$, and CdS_2O_3 coordination geometries, respectively. Note that two neighboring elements in the periodic table (such as oxygen and nitrogen) with very similar amplitude functions cannot be distinguished by EXAFS.

The structural parameters were refined by least-squares methods, fitting the model function $\chi(k)$ to the experimental unfiltered EXAFS oscillation using k^3-weighting, generally over the k range 3−14 Å^{-1}, allowing the bond distance (R), Debye−Waller parameter (σ), and ΔE_0 (with a common value for all scattering paths) to float, while the amplitude reduction factor (S_0^2) and/or coordination number (N) were fixed. The S_0^2 value refined to 0.99 at the EXAFS data analysis for crystalline $[Cd(TU)_4](NO_3)_2$ with the coordination number fixed (4 Cd−S; Figure S-7). This parameter value was then kept fixed at 1.0

dx.doi.org/10.1021/ic300852t | Inorg. Chem. 2012, 51, 10619−10630

Table 4. Structural Parameters Derived from EXAFS Least-Squares Curve Fitting for the Cd(II)−SeU Methanol Solutions S1 and S5 at 200 K ($C_{Cd(II)}$ ∼ 0.1 mol dm^{-3}; see Figure 3)[a]

	Cd−O			Cd−Se			
solution (SeU/Cd(II))	N	R (Å)	σ^2 (Å^2)	N	R (Å)	σ^2 (Å^2)	$\mathcal{R}^b$
S1 (1.0)	5 f	2.29	0.0066	1 f	2.62	0.0036	18.0
S5 (5.0)				3.8	2.63	0.0043	24.4

[a]Fitting k-range = 3−14 Å^{-1}; S_0^2 = 1.0 f (f = fixed); estimated error limits: N ± 20%, R ± 0.02 Å, σ^2 ± 0.001 Å^2. [b]Residual; the residual (%) from the least-squares curve fitting is defined as follows:

$$\frac{\sum_{i=1}^{N} |y_{exp}(i) - y_{theo}(i)|}{\sum_{i=1}^{N} |y_{exp}(i)|} \times 100$$

where y_{exp} and y_{theo} are k^3-weighted experimental and theoretical data points, respectively.

during the EXAFS curve-fitting process for the solutions (Tables 4, 5, and S-2). The accuracy of the refined coordination numbers N, bond distances R, and their Debye−Waller parameters (σ^2) for the dominating Cd−Se and Cd−S paths is estimated to be within ±20%, ±0.02 Å, and ±0.001 Å^2, respectively, accounting for effects of systematic deviations in the extracted data, model limitations, correlated parameters, etc. The above error limits were estimated from variations in the parameter values when refining models of different complexity, when systematically varying the k-range, or when trying different cubic spline removals. The corresponding structural parameters for the Cd−O path are less accurate, ±0.04 Å for bond distances (±0.02 Å for SeU complexes) and ±0.002 Å^2 (±0.001 Å^2 at LT) for Debye−Waller parameters σ^2, due to the difficulties associated with separating the EXAFS contribution from the oxygen (or nitrogen) atoms, when their mean bond distance is rather close to that of the heavier sulfur atoms.

To the experimental LT EXAFS spectra of solutions **T6** and **T7**, linear combinations of simulated EXAFS oscillations for CdS_4 and CdS_6 coordination were fitted in the k range 3.4−14.4 Å^{-1}, following a procedure explained elsewhere,[76] with the S_0^2 and ΔE_0 values fixed at 1.0 and 1.0 eV, respectively. The simulations were performed for CdS_4 by varying the average Cd−S distance in the range 2.53−2.54 Å (σ^2 = 0.005−0.007 Å^2) and for CdS_6, 2.68−2.74 Å (σ^2 = 0.006−0.007 Å^2). The best fits were obtained with the following parameters: CdS_4 (4 Cd−S, R = 2.54 Å, σ^2 = 0.005 Å^2) and CdS_6 (6 Cd−S, R = 2.71 Å, σ^2 = 0.007 Å^2).

RESULTS

^{113}Cd NMR Spectroscopy. ^{113}Cd NMR spectra were measured at 203 K of 0.1 mol dm^{-3} dehydrated $Cd(CF_3SO_3)_2$ in methanol solutions (30% CD_3OD) containing different concentrations of thiourea (**T1**−**T7**) or selenourea (**S1**−**S5**) (see Figure 1 *left* and *middle*). The spectrum of $Cd(CF_3SO_3)_2$ in methanol without added ligands (L = TU, SeU) showed a signal at −21 ppm. In the solutions **S1** and **T1**, both with the mole ratio L/Cd(II) = 1.0, several sharp signals with similar ^{113}Cd chemical shifts appeared. A small peak at −21 ppm showed that at this mole ratio some Cd(II) ions still remained free; however, at increasing ligand concentration, this signal disappeared. For the methanol solutions **S2**−**S3** and **T2**−**T3** with L/Cd(II) mole ratios 2.0 and 3.0 (L = TU, SeU), respectively, up to five distinct ^{113}Cd NMR signals appeared, indicating four Cd(II) species with different coordination environments in slow ligand-exchange equilibria, beside the solvated Cd^{2+} ion.

The first two sharp signals appeared with very similar chemical shifts: 94 and 191 ppm for **T2** and **T3**, versus 97 and 194 ppm for **S2** and **S3**, while the next two signals were broader and more shielded for the Cd(II)-thiourea solutions **T2** and **T3** (333 and 526 ppm) than for the Cd(II)-selenourea solutions **S2** and **S3** (435 and 578 ppm). For solutions **S4** and **S5**, only one single sharp signal at 578 ppm remained, corresponding to a single dominating Cd(II)−selenourea complex. Also, the Cd(II) thiourea solutions **T4**−**T7** displayed a single, relatively broad peak. However, the gradual increase in shielding from 515 ppm in **T4** to 423 ppm in **T7** with increasing thiourea concentration can be attributed to a gradual change in the coordination environment around Cd(II).

Table 5. Structural Parameters Derived from EXAFS Least-Squares Curve Fitting of Models for the Cd(II)-TU Methanol Solutions T1, T2, and T4−T7 at 200 K (LT) and 298 K (RT) ($C_{Cd(II)}$ ∼ 0.1 mol dm^{-3}; see Figure 4)[a]

		Cd−S			Cd−O			
solution (TU/Cd(II) mole ratio)	^{113}Cd δ (ppm)	N	R (Å)	σ^2 (Å^2)	N	R (Å)	σ^2 (Å^2)	$\mathcal{R}^b$
$[Cd(TU)_4](NO_3)_2$ solid	577 (δ_{iso})	4 f	2.53	0.0063				15.4
Temp 200 K								
T1 (1.0)	−21, 93 (major), 189	1 f	2.54	0.0030	5 f	2.30	0.0047	17.4
T2 (2.0)	94, 191 (major), 337	2 f	2.55	0.0056	4 f	2.33	0.0062	14.3
T4 (4.0)	515 (broad)	3.8	2.53	0.0052				13.9
T5 (5.0)	506	3.8	2.54	0.0057				13.4
T6 (8.0)	458	3.3	2.54	0.0066				22.2
T7 (10.0)	423	3.8	2.55	0.0087				20.6
Temp 298 K								
T1 (1.0)		1 f	2.54	0.0063	5 f	2.30	0.0075	14.2
T2 (2.0)		2 f	2.51	0.0066	4 f	2.34	0.0132	18.2
T4 (4.0)	503	3.3	2.52	0.0060				8.1
T5 (5.0)	534	3.3	2.53	0.0057				10.7
T6 (8.0)	541	3.3	2.53	0.0053				13.9
T7 (10.0)	533	3.5	2.53	0.0063				10.1

[a]k-range for fitting 3−14 Å^{-1}; S_0^2 = 1.0 f (f = fixed) for solutions; estimated error limits: N ± 20%, for Cd−S R ± 0.02 Å, σ^2 ± 0.001 Å^2; for Cd−O R ± 0.04 Å and σ^2 ± 0.002 Å^2. [b]Residual.

dx.doi.org/10.1021/ic300852t | Inorg. Chem. 2012, 51, 10619−10630

The ^{113}Cd NMR spectra obtained for the thiourea solutions **T4**−**T7** at room temperature are shown in Figure 1 (*right*). No signal could be obtained for **T1**−**T3**, since the ^{113}Cd NMR signals became broader and finally disappeared at 223 K. For solutions **T4**−**T7**, the single ^{113}Cd NMR signal became considerably sharper and mostly less shielded at RT, which means either that a single dominating Cd(II) thiourea complex is present or that the Cd(II)−thiourea species are in fast ligand exchange.

To investigate the influence of the solvent on the Cd(II)−thiourea complex formation, ^{113}Cd NMR spectra were measured of a series of aqueous 0.1 mol dm^{-3} $Cd(CF_3SO_3)_2$ solutions with different TU/Cd(II) mole ratios (Figure 2). All

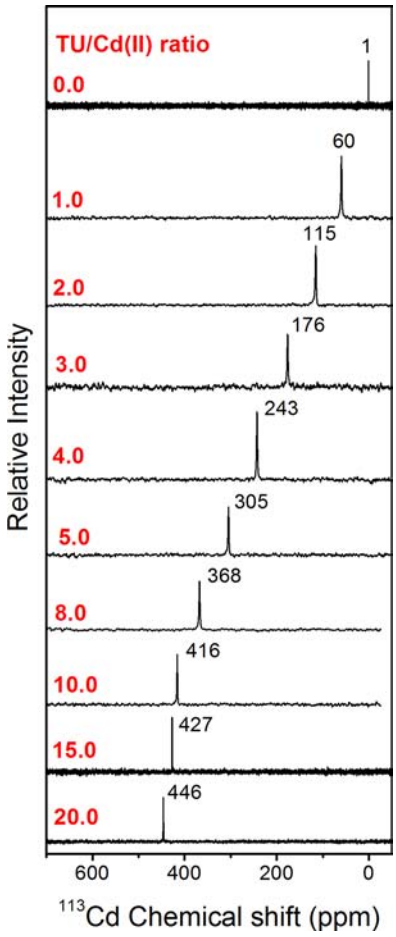

Figure 2. ^{113}Cd NMR spectra of 0.1 mol dm^{-3} $Cd(CF_3SO_3)_2$ aqueous solutions (**W1**−**W9**) with thiourea mole ratios TU/Cd(II) increasing from 1.0 to 20.0, measured at 295 K; see Table 3. The spectrum at the top is for a solution without added thiourea.

spectra showed a single sharp signal, which with increasing ligand concentration gradually became less shielded, from $\delta(^{113}Cd)$ = 1 ppm for 0.1 mol dm^{-3} $Cd(CF_3SO_3)_2$ in aqueous solution, 60 ppm with 0.1 mol dm^{-3} thiourea in **W1**, to 446 ppm for 2.0 mol dm^{-3} thiourea in **W9** (mole ratio TU/Cd(II) = 20), indicating that S ligand atoms gradually replace O atoms in the Cd(II) coordination environment.

X-ray Absorption Spectroscopy—Cd K-Edge EXAFS. Cd K-edge EXAFS spectra were measured at 200 K for the methanol solutions **S1** and **S5** with the SeU/Cd(II) mole ratios 1.0 and 5.0, respectively (Figure 3); the curve-fitting results are shown in Table 4. Solutions **S2**, **S3**, and **S4** were not measured, since

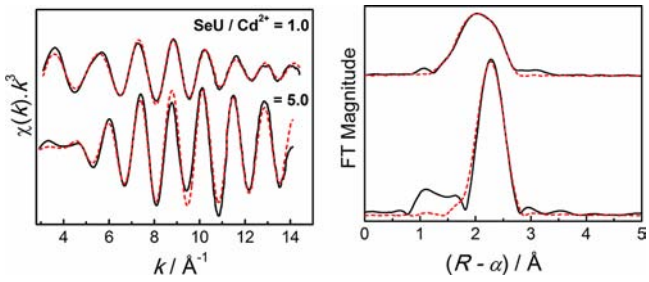

Figure 3. Cd K-edge EXAFS curve-fitting for the Cd(II)-selenourea methanol solutions **S1** and **S5** with SeU/Cd(II) mole ratios 1.0 and 5.0 ($C_{Cd(II)}$ = 0.1 mol dm^{-3} measured at 200 K (see Table 4)).

the ^{113}Cd NMR measurements showed that solutions **S2**−**S3** contained mixtures of Cd(II)−SeU complexes and that the speciation was similar in solution **S4** as in **S5**. Also, solution **S1** contained several Cd(II)−SeU complexes, with the dominating one giving a signal at $\delta(^{113}Cd)$ = 96 ppm (Figure 1, *left*). The EXAFS oscillation of this solution was well fitted with a model containing one SeU ligand and five oxygen donors from solvent (methanol) molecules and possibly also the $CF_3SO_3^-$ anion, with average Cd−Se and Cd−O bond distances of 2.62 ± 0.02 Å and 2.29 ± 0.02 Å, respectively. This model is supported by a calculation of the average number of bound SeU per Cd(II) ion (=1.01) from the ^{113}Cd NMR peak integrals, which corresponds to the fraction of each Cd(II) complex in solution **S1** (Appendix 1, Supporting Information). The EXAFS oscillation of solution **S5** with considerably higher amplitude than that of **S1** was well modeled by four Cd−Se paths at 2.63 ± 0.02 Å (Table 4).

For the series of Cd(II) thiourea solutions **T1**−**T7** (excluding **T3**) in MeOH, Cd K-edge EXAFS spectra were measured at both 200 K (LT) and 298 K (RT), as shown in Figure 4. Based on the ^{113}Cd NMR spectrum of solution **T1** at 203 K, a mono(thiourea) cadmium(II) complex with δ = 93 ppm dominates in this solution, together with a minor amount of solvated Cd^{2+} ions and $Cd(TU)_2^{2+}$ species (see below). Least squares curve-fitting to the k^3-weighted EXAFS oscillation of **T1** at LT with a model consisting of one Cd−S and five Cd−O scattering paths resulted in the mean distances 2.54 ± 0.02 Å and 2.30 ± 0.04 Å, respectively (Table 5). The number of bound TU/Cd(II) (=1.06) from the peak integrals in the ^{113}Cd NMR spectrum of solution **T1** (Figure 1, *middle*) supports this model; see Appendix 2 in the Supporting Information.

When increasing the thiourea concentration to 0.2 mol dm^{-3} in solution **T2** (mole ratio TU/Cd(II) = 2.0), the ^{113}Cd NMR spectrum indicated two major Cd(II) thiourea complexes with $\delta(^{113}Cd)$ = 94 and 191 ppm beside a minor peak at 337 ppm (Figure 1). The FT peak position for the LT EXAFS spectrum for this solution shifted slightly to a longer distance and gained intensity (Figure 4). The LT EXAFS oscillation of this solution could be modeled with 2 Cd−S (2.55 ± 0.02 Å) and 4 Cd−O (2.33 ± 0.04 Å) scattering paths (Table 5). The peak integrals in the ^{113}Cd NMR spectrum of solution **T2** (Figure 1, *middle*) correspond to 2.17 bound TU/Cd(II) (see Appendix 2, Supporting Information). This ratio is higher than the stoichiometric TU/Cd(II) ratio (2.0), indicating an error of about 10% in the number estimated from the peak integrals. The EXAFS oscillation for solution **T3** was not analyzed, as it contained several Cd(II) thiourea species beside the dominating one with $\delta(^{113}Cd)$ = 191 ppm (Figure 1).

dx.doi.org/10.1021/ic300852t | *Inorg. Chem.* 2012, 51, 10619−10630

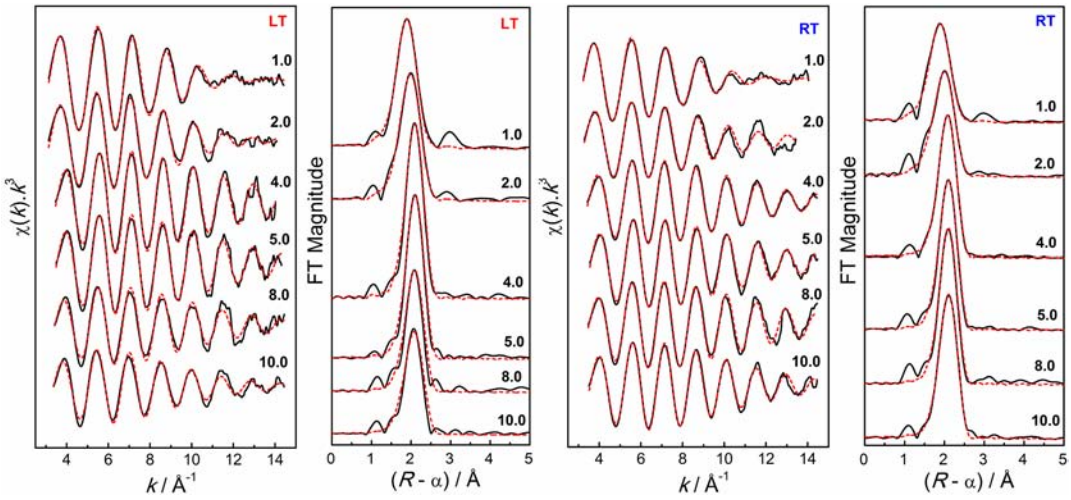

Figure 4. Cd K-edge EXAFS (black lines) and curve-fitted model (red dashes) oscillations and corresponding Fourier-transforms for Cd(II)−thiourea complexes in methanol solutions ($C_{Cd(II)}$ = 0.1 mol dm^{-3}) with the mole ratios TU/Cd(II) 1.0 (**T1**), 2.0 (**T2**), 4.0 (**T4**), 5.0 (**T5**), 8.0 (**T6**), and 10.0 (**T7**) measured at 200 K (LT) and 298 K (RT); see Table 5.

The highest FT amplitude in the LT EXAFS series **T1**−**T7** was obtained for solutions **T4** and **T5** with $\delta(^{113}Cd)$ = 515 and 506 ppm, respectively. The LT EXAFS oscillations of these solutions were well modeled with four Cd−S distances at 2.53−2.54 Å. Attempts to include a Cd−O path resulted in too short Cd−O bond distances and/or unreasonable disorder parameters. With further increase in the thiourea concentration, from 0.5 mol dm^{-3} in **T5** to 1.0 mol dm^{-3} in **T7**, the single ^{113}Cd NMR signal shifted upfield from $\delta(^{113}Cd)$ = 506 ppm to 423 ppm (Figure 1), with a considerable amplitude reduction of the LT EXAFS oscillations, as shown in Figure S-5 for solutions **T4** and **T7** with the TU/Cd(II) mole ratios 4.0 and 10.0, respectively. This figure also shows that at 298 K the EXAFS spectra of these solutions (**T4** and **T7**) overlap, which is consistent with their similar sharp ^{113}Cd NMR peaks at 503 and 533 ppm, respectively (Figure 1, *right*), indicating that at room temperature the difference in speciation is not large enough to be distinguished by EXAFS spectroscopy.

The RT EXAFS oscillations for solutions **T4**−**T7** were well modeled with four Cd−S paths at 2.53 ± 0.02 Å (Table 5). A comparison of the EXAFS oscillations measured for solution **T4** at two different temperatures (Figure S-6) shows similar frequencies, reflected in their similar bond distances (2.52−2.53 Å). However, the amplitude is higher at LT, resulting in slightly higher N_{Cd-S} (with fixed S_0^2) and smaller σ^2 values in the refinements. For solutions **T1** and **T2**, for which no ^{113}Cd NMR signal could be observed at RT, the EXAFS spectra had smaller amplitude at RT than at LT; see Figure S-6. For solution **T2**, the LT EXAFS oscillation had higher frequency, showing a significant shift to longer Cd−S bond distances from 2.51 Å at RT to 2.55 Å at LT, while the change in temperature did not influence the mean Cd−S and Cd−O bond distances for solution **T1** (Table 5).

Cd K-edge EXAFS spectra for the Cd(II) thiourea aqueous solutions **W1**−**W7** were also measured and analyzed assuming mixtures of hydrated $Cd(TU)_x^{2+}$ (x = 1−4) species; see Figure S-1 and Table S-2.

X-ray Absorption Spectroscopy—Cd L_3-Edge XANES. Cd L_3-edge XANES spectroscopy has been shown to be sensitive to the type of coordinating atoms and the local coordination geometry around the cadmium(II) ion in its complexes. For example, Cd(II) complexes with CdO_6 octahedral geometry show a distinct pre-edge feature at 3539.1 eV, originating from a core electron transition from Cd $2p_{3/2}$ to higher unoccupied molecular orbitals with s or d character.[77−79] Therefore, Cd L_3-edge XANES spectra were measured at room temperature of the Cd(II) thiourea solutions in methanol (**T1**−**T7**) including $Cd(CF_3SO_3)_2$ (model for CdO_6), and for crystalline compounds with different CdS_xO_y coordination geometries (Figure 5). The XANES spectrum of solution **T1** with a distinct pre-edge feature at 3539.1 eV resembles that of CdO_6, while the second derivative of the spectral features for **T2** is similar to

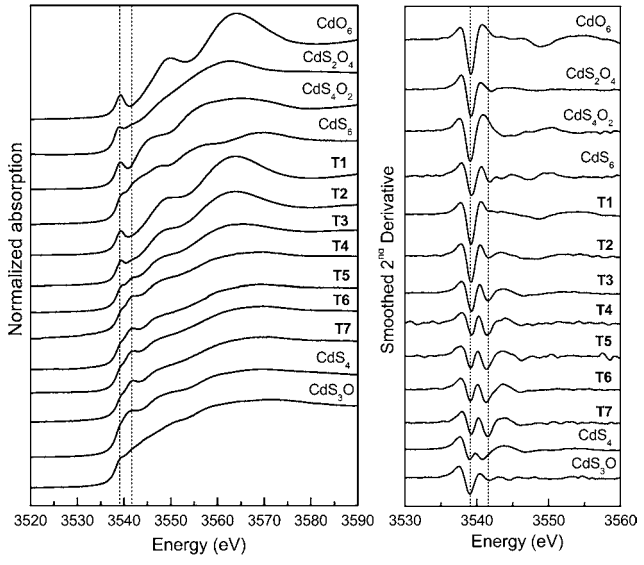

Figure 5. Cd L_3-edge XANES spectra at RT of the Cd-$(CF_3SO_3)_2$thiourea solutions in methanol **T1**−**T7**, compared with $Cd(CF_3SO_3)_2$ in methanol (CdO_6) and crystalline standard compounds with CdS_xO_y coordination:[79] $[Cd(tmtu)_2(NO_3)_2]$ (CdS_2O_4 model; tmtu = tetramethylthiourea),[80] $[Cd(DMTF)_4(CF_3SO_3)_2]$ (CdS_4O_2 model),[48] $[Cd(DMTF)_6](ClO_4)_2$ (CdS_6 model),[48] cadmium adamantane cage $(Et_3NH)_4[S_4Cd_{10}(SPh)_{16}]$ (CdS_4 model),[53] and $(HIm)[Cd(tsac)_3(H_2O)]$ (CdS_3O model; tsac = thiosaccharinato).[49] The dashed lines are at 3539.1 and 3541.6 eV.

dx.doi.org/10.1021/ic300852t | *Inorg. Chem.* 2012, 51, 10619−10630

those of CdS_2O_4. For solutions **T4**−**T7**, the Cd L_3-edge XANES features and corresponding second derivatives are very similar, and comparable to the CdS_4 model.

DISCUSSION

Selenourea Cd(II) Complex Formation. The combined results from the ^{113}Cd NMR and Cd K-edge EXAFS spectroscopic studies show a dominating monoselenourea $Cd(SeU)^{2+}$ complex with $CdSeO_5$ coordination in the methanol solution **S1** with mole ratio SeU/Cd(II) = 1.0 (see Figures 1, 3, and Table 4). The O-donor ligands are methanol molecules and triflate ions, as in $[Cd(DMTF)_4(CF_3SO_3)_2]$.[48] For the mole ratios SeU/Cd(II) = 4.0 and 5.0 (solutions **S4** and **S5**, respectively), a single cadmium(II)−selenourea complex $[Cd(SeU)_4]^{2+}$ with $\delta(^{113}Cd)$ = 578 ppm dominates. The mean Cd−Se bond distance of 2.63 ± 0.02 Å (Table 4) is compatible with the average Cd−Se bond distances of 2.649 Å in $[N(CH_3)_4]_2[Cd(SePh)_4]$[81] and 2.623 Å in $[Cd(dmise)_4][PF_6]_2$, the only crystal structures with homoleptic $CdSe_4$ coordination geometry.[74] The synthesis of $[Cd(SeU)_4]SO_4$ was reported in 1972 without structural information.[82] The ^{113}Cd NMR chemical shift, 541 ppm, for the $[Cd(SePh)_4]^{2+}$ complex in methanol solution at 213 K[59] is slightly more shielded than that reported here of the $[Cd(SeU)_4]^{2+}$ complex at 203 K ($\Delta\delta$ = 578−541 = 37 ppm).

The slow ligand-exchange for the methanol solutions **S1**, **S2**, and **S3** at 203 K allows the peaks observed at $\delta(^{113}Cd)$ = 96−97, 193−194, 435, and 578 ppm (Figure 1) to be assigned to complexes with $CdSeO_5$, $CdSe_2O_4$, $CdSe_3O$, and $CdSe_4$ coordination, respectively. The relatively broad peaks prevented ^{113}Cd−^{77}Se coupling to be observed; such one-bond coupling normally is within 50−200 MHz.[64] Previously, a ^{113}Cd chemical shift of 250 ppm was obtained for a cadmium(II) selenocarboxylate complex with trigonal bipyramidal $CdSe_3O_2$ coordination geometry in CH_2Cl_2 at 193 K.[64] A CSD survey did not show any crystalline compound with $CdSe_2O_4$ coordination, only one Cd(II) complex with $CdSe_2O_3$ coordination,[83] and one monomeric $CdSe_3O$ complex with the Cd−Se bond distances within 2.590−2.603 Å and Cd−OH_2 at 2.307 Å.[84]

By assuming that the integrated area of a distinct ^{113}Cd NMR peak in Figure 1 is proportional to the concentration of a specific Cd(II) species in each cadmium(II)−selenourea (**S1**−**S3**) solution, the relative fractions (%Cd) and the formation constants of the Cd(II) species were evaluated (Table S-1b, Supporting Information). The formation constants ($\log \beta_x$, x = 1−4) of the $Cd(SeU)_x^{2+}$ species above were varied systematically until the distribution of complexes calculated in fraction diagrams approximately agreed with those obtained from the ^{113}Cd NMR spectra; see Figure S-8 (*top*) in Appendix 1, Supporting Information. The evaluation showed that the $\log \beta_x$ values are correlated with an estimated error limit of ±0.5 logarithmic units (Table 6).

Thiourea Cd(II) Complex Formation in MeOH. Low Temperature (~200 K). In the ^{113}Cd NMR spectra of the methanol solutions with TU/Cd(II) mole ratios 1.0, 2.0, and 3.0 (**T1**, **T2**, and **T3**), four peaks appeared at 203 K with δ = 93−94, 189−191, 333−337, and 526 ppm (Figure 1). A similar observation was reported for methanol solutions of $Cd(ClO_4)_2$ and 1,3-thiazolidine-2-thione (tztH) at 189 K with four peaks at −14, 73, 153, and 453 ppm, which were tentatively assigned to solvated $[Cd(tztH)_w]^{2+}$ complexes with w = 0−3, respectively.[46] For solution **T1**, the peak at 93 ppm has the highest intensity, and its Cd K-edge EXAFS spectrum is well modeled with one Cd−S and five Cd−O bond distances (2.54 ± 0.02 and 2.30 ± 0.04 Å, respectively; see Figure 4 and Table 5), showing that a mono(thiourea) Cd(II) complex with $CdSO_5$ coordination (O from MeOH or $CF_3SO_3^-$) dominates. For the methanol solution **T2** with $C_{Cd(II)}$ = 0.1 mol dm^{-3} and C_{TU} = 0.2 mol dm^{-3}, the ^{113}Cd NMR signal at 191 ppm is the most intense (Figure 1). The average Cd−S and Cd−O bond distances 2.55 ± 0.02 Å and 2.33 ± 0.04 Å (Table 5) are comparable with the average Cd−S (2.585 Å) and Cd−O (2.366 Å) distances for the *cis*-$[Cd(TU)_2(H_2O)_4](SO_4)$ complex,[52] for which an isotropic solid state ^{113}Cd NMR chemical shift of 148 ppm was observed (Figure S-4b). We conclude that a bis(thiourea)cadmium(II) complex, $Cd(TU)_2^{2+}$, with a CdS_2O_4 coordination environment dominates in solution **T2**.

In solution **T3** (TU/Cd(II) mole ratio =3.0), several species are in equilibrium, giving rise to two sharp ^{113}Cd NMR signals at 94 ppm ($CdSO_5$) and 191 ppm (CdS_2O_4) and two broad peaks at 333 ppm and 526 ppm (Figure 1). The reported isotropic ^{113}Cd NMR chemical shifts for complexes with CdS_3O_2 and CdS_3O_3 coordination (S = thiolate) vary within the range δ_{iso} = 390−410 ppm.[85,86] Considering that the $(HIm)[Cd(tsac)_3(H_2O)]$ and $[Cd(TU)_3(SO_4)]$ complexes with CdS_3O coordination showed isotropic solid state ^{113}Cd NMR chemical shifts at 378 and 346 ppm at room temperature, respectively (Figure S-4a, b), we can assign the peak at 333 ppm to tris(thiourea) Cd(II) complexes with CdS_3O_{1-3} coordination in relatively fast ligand-exchange that broadens the peak. The broad peak at 526 ppm in the NMR spectrum of solution **T3** can be assigned to a tetra(thiourea) Cd(II) complex mainly with CdS_4 coordination (see the Room Temperature section).

Similar to the Cd(II)−selenourea system, the integrated peak areas in the ^{113}Cd NMR spectra of the methanol solutions **T1**−**T3** at 203 K (Figure 1) were used to estimate the concentration of $Cd(TU)_y^{2+}$ (y = 1−4) species in each solution (Appendix 2, Supporting Information). The formation constants $\log \beta_y$ were varied until the calculated fractions of $Cd(TU)_y^{2+}$ species in Figure S-9 (*top*) closely matched the fractions obtained from the peak areas (Table 6). The resulting β_y values obtained for the solvated $Cd(TU)_y^{2+}$ (y = 1−4) species in methanol at 203 K ($\beta_1 = 2.0 \times 10^4$, $\beta_2 = 2.0 \times 10^7$, $\beta_3 = 5.0 \times 10^9$, and $\beta_4 = 2.5 \times 10^{12}$) differ considerably from those previously reported from a polarographic study for similar complexes in aqueous solution at 298 K (β_1 = 20, β_2 = 140, β_3 = 260, and β_4 = 1200).[16]

By increasing the thiourea concentration from 0.4 mol dm^{-3} in **T4** to 1.0 mol dm^{-3} in **T7** ($C_{Cd(II)}$ = 0.1 mol dm^{-3}), the single ^{113}Cd NMR peak became more shielded, shifting from 515 ppm in **T4** to 423 ppm in **T7**. The latter value can be

Table 6. Formation Constants[a] of the Cd(II) Selenourea/Thiourea Species CdL_x^{2+} (L = SeU/TU, x = 1−4) Formed in Methanol Solutions, Derived from ^{113}Cd NMR Spectra at 203 K (See Figures 1, S-8, and S-9)

	$\log \beta_x$ (SeU)	$\log \beta_x$ (TU)
CdL^{2+}	4.4	4.3
CdL_2^{2+}	7.3	7.3
CdL_3^{2+}	10.7	9.7
CdL_4^{2+}	14.0	12.4

[a] $\beta_x = [CdL_x^{2+}]/([Cd^{2+}][L]^x)$.

compared with $\delta_{iso}(^{113}Cd)$ = 402 ppm recorded for crystalline $[Cd(DMTF)_6](ClO_4)_2$ with octahedral CdS_6 coordination (see Figure S-3). Therefore, the gradual shift of the NMR signal from 515 to 423 ppm is probably due to partial formation of Cd(II) complexes with a higher number of coordinated thiourea ligands, e.g. $[Cd(TU)_5]^{2+}$ (CdS_5) and octahedral $[Cd(TU)_6]^{2+}$ (CdS_6) species. Even though solution **T7** has the highest thiourea concentration, the amplitude of its LT EXAFS oscillation is visibly smaller than that for **T4** (Figure S-5 *left*).

An attempt to evaluate the speciation of the higher Cd(II)−thiourea complexes was made by fitting the LT EXAFS spectra for solutions **T6** and **T7** (TU/Cd(II) mole ratios 8.0 and 10.0, respectively) with linear combinations of EXAFS oscillations simulated for CdS_4 and CdS_6 coordination. The best fits shown in Figure 6 were obtained with the mean Cd−S distances 2.54

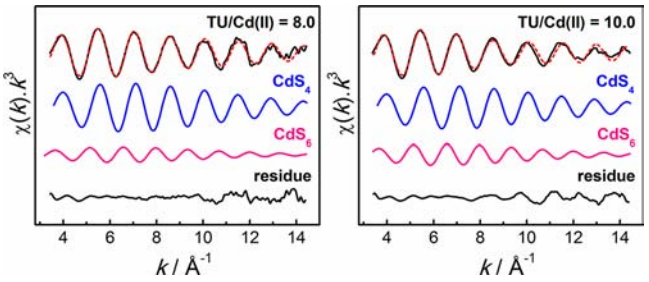

Figure 6. Cd K-edge EXAFS spectra at LT for the Cd(II) thiourea methanol solutions **T6** and **T7** fitted with linear combinations of simulated EXAFS oscillations for CdS_4 and CdS_6 coordination, indicating more than four thiourea ligands in ∼20−30% of the cadmium(II) complexes.

Å (σ^2 = 0.005 Å^2) for CdS_4 and 2.71 Å (σ^2 = 0.007 Å^2) for CdS_6, which are comparable with the mean Cd−S distance in crystalline $[Cd(TU)_4](NO_3)_2$ with CdS_4 coordination (2.53 ± 0.02 Å from EXAFS; Table 5 and Figure S-7) and 2.711 Å in a crystalline $[Cd(TU)_6]^{2+}$ complex with CdS_6 coordination.[15] Note that while the average of the crystallographic Cd−S distances in $[Cd(TU)_4](NO_3)_2$ is 2.560 Å,[13] the slightly shorter EXAFS value 2.53 ± 0.02 Å could result from a higher contribution from its short, more well-defined bond distances to the EXAFS oscillation. Ignoring a possible contribution from $Cd(TU)_5^{2+}$ species, the linear combination fitting results in a 77% contribution from CdS_4 and 23% from CdS_6 to the EXAFS oscillation for solution **T6**; for solution **T7** the contributions are 68% CdS_4 and 32% CdS_6 (estimated error ±10%). Figure 6 shows that the amplitude of the experimental EXAFS spectra is reduced by the opposing phases of the EXAFS oscillations for CdS_4 and CdS_6 coordination. Such a change in the Cd(II) speciation as in these solutions would have been difficult to interpret solely based on EXAFS spectroscopy, without the aid from the ^{113}Cd NMR spectra.

Room Temperature. For the cadmium(II) thiourea solutions **T1**−**T3**, for which no ^{113}Cd NMR signal could be observed at 295 K, the Cd L_3-edge XANES spectral features were useful for indicating the coordination of the major cadmium(II) species. The Cd L_3-edge XANES spectrum of **T1** resembles that of $Cd(CF_3SO_3)_2$ in methanol (CdO_6 model) in Figure 5. At LT the ^{113}Cd NMR spectrum showed that some free solvated Cd^{2+} ions were present (Figure 1). The RT EXAFS spectrum of solution **T1** could be fitted with a $CdSO_5$ model with the average Cd−O and Cd−S distances 2.30 ± 0.02 Å and 2.54 ± 0.02 Å, respectively, which are comparable to those obtained for this solution at LT (see Table 5 and Figure S-6). The resemblance between the Cd L_3-edge XANES spectra of solution **T2** and the CdS_2O_4 model in Figure 5, and also the corresponding second derivatives, implies that solution **T2** mainly contains the bis(thiourea)cadmium(II) complex as the dominating species. Fitting the RT Cd K-edge EXAFS spectrum of solution **T2** with a CdS_2O_4 model resulted in a somewhat shorter average Cd−S distance 2.51 ± 0.02 Å.

The ^{113}Cd NMR spectra of solutions **T4**−**T7** with TU/Cd(II) mole ratios 4.0−10.0 showed at 295 K a single sharp peak in the 503−541 ppm region. The RT EXAFS spectra of these solutions almost overlap (Figure S-5, *right*) and were well fitted with a CdS_4 model with an average Cd−S distance of 2.52−2.53 Å. The second derivatives of their Cd L_3-edge absorption spectra showed two minima, rather similar to those observed for the CdS_4 model compound (Figure 5). Thus, at high thiourea concentration (TU/Cd(II) > 4.0) the $[Cd(TU)_4]^{2+}$ complex dominates at room temperature. Reducing the temperature of these solutions (**T5**−**T7**) to ∼200 K promotes the formation of CdS_{5-6} complexes, resulting in longer average Cd−S distances (up to 2.55 Å for **T7**) and more shielded ^{113}Cd chemical shifts (423 ppm for **T7**).

For the crystalline $[Cd(TU)_4](NO_3)_2$ complex with an average Cd−S distance of 2.53 ± 0.02 Å (from EXAFS; see Table 5 and Figure S-7), a solid state ^{113}Cd NMR isotropic chemical shift of δ_{iso} = 577 ppm was obtained (Figure S-3), while the ^{113}Cd NMR chemical shift for $[Cd(TU)_4]^{2+}$ ions in methanol solution is more shielded (541 ppm at 295 K). A similar upfield shift has been reported for $[Cd(Se\text{-}2,4,6\text{-}^iPr_3\text{-}C_6H_2)_2(bpy)]$ complex (δ_{iso} = 460, 472) when dissolved in chloroform (411 ppm)[61] and was explained as a "solvent effect" (see Table 2).

Based on the above discussion, the broad peak at 526 ppm in the LT ^{113}Cd NMR spectrum of solution **T3** can be assigned to $[Cd(TU)_4]^{2+}$ species with rather slow ligand-exchange on the NMR scale. The broadness of this peak could be due to a minor amount of a Cd(II) tetra(thiourea) complex with CdS_4O coordination. Higher O-donor ligand coordination is not likely, since the chemical shift becomes more shielded, e.g. for $[Cd(DMTF)_4(CF_3SO_3)_2]$ with CdS_4O_2 coordination, δ_{iso} (^{113}Cd) = 267 ppm (Table 1). The isotropic chemical shifts for CdS_4 and CdS_4O coordination (S = thiolate) in the $[Cd_{10}(SCH_2CH_2OH)_{16}](ClO_4)_4$ compound were reported at 674 and 503 ppm, respectively.[87] The sign of the chemical shifts is changed; also, the calibration is shifted by changing δ_{iso} for the solid reference compound $Cd(NO_3)_2{\cdot}4H_2O$ from 0.0 ppm to −100 ppm. The ^{113}Cd NMR chemical shifts measured at room temperature for the $[Cd(TU)_4]^{2+}$ complex (CdS_4 coordination) in the solid state (δ_{iso} = 577 ppm) and in methanol solution (541 ppm) are more shielded than that for mononuclear Cd(II)−tetrathiolate complexes (∼600−750 ppm).[43]

Thiourea Cd(II) Complex Formation in H_2O. The cadmium(II) complex formation with thiourea in aqueous solution was also investigated at room temperature, keeping the same cadmium(II) concentration as for the methanol solutions (∼0.1 mol dm^{-3} $Cd(CF_3SO_3)_2$), with the TU concentration varying from 0.1 to 2.0 mol dm^{-3} (**W1**−**W9**, Table 3). The single sharp peak with a gradual downfield shift from 60 ppm (**W1**) to 446 ppm (**W9**) in the ^{113}Cd NMR spectra shown in Figure 2 corresponds to cadmium(II) complexes with an increasing number of coordinated thiourea ligands in fast ligand exchange, as the TU concentration increases. A similar trend is

dx.doi.org/10.1021/ic300852t | *Inorg. Chem.* 2012, 51, 10619−10630

also observed for the isotropic ^{113}Cd NMR chemical shifts with δ_{iso} = 148, 346, and 577 ppm of the *cis*-$[Cd(TU)_2(H_2O)_4](SO_4)$, $[Cd(TU)_3(SO_4)]$, and $[Cd(TU)_4](NO_3)_2$ solid compounds, respectively (Table 1).

The Cd K-edge EXAFS spectra for the aqueous solutions **W1**−**W7** were analyzed (Table S-2), keeping the average Cd−S and Cd−O coordination numbers fixed at values derived from the calculated distribution of complexes assuming $[Cd(TU)_y(H_2O)_{6-y}]^{2+}$ (y = 0−3) and $[Cd(TU)_4]^{2+}$ species (Figure S-1); the results showed a mean Cd−S distance of about 2.54−2.57 Å for solutions **W1** to **W5**. The mean Cd−S distance became slightly shorter, about 2.53 Å, for solutions **W6** and **W7** (TU/Cd mole ratios 8.0 and 10.0, respectively), while the mean of the Cd−O distances is around 2.28 ± 0.04 Å for all solutions (Table S-2). This trend corresponds to that expected for hydrated $[Cd(TU)(H_2O)_5]^{2+}$ and $[Cd(TU)_2(H_2O)_4]^{2+}$ complexes in a mixture, with a gradually increasing amount of $[Cd(TU)_4]^{2+}$ complexes without coordinated water (Figure S-1). The crystal structure of a hydrated cadmium thiourea sulfate showed both *cis*-$[Cd(TU)_2(H_2O)_4](SO_4)$ and *fac*-$[Cd(TU)_3(H_2O)_3](SO_4)$ complexes cocrystallized in the unit cell, with the mean Cd−S (Cd−O) bond distances 2.59 (2.37) Å and 2.62 (2.41) Å, respectively.[52] A mean Cd−S distance of 2.53 ± 0.02 Å is expected for a $[Cd(TU)_4]^{2+}$ complex from EXAFS, as obtained for the solid $[Cd(TU)_4](NO_3)_2$ compound (Table 5 and Figure S-7).

Therefore, we interpret the combined results of the aqueous solutions **W1**−**W5** ($C_{Cd(II)}$ = 0.1 mol dm^{-3} and TU/Cd(II) = 1.0−5.0) as corresponding to dominating hydrated $[Cd(TU)(H_2O)_5]^{2+}$ and $[Cd(TU)_2(H_2O)_4]^{2+}$ complexes that are in fast ligand exchange on the NMR time scale. By further increasing the thiourea concentration in solutions **W6** to **W9** (mole ratios TU/Cd(II) = 8.0−20.0, respectively), the tetrahedral $[Cd(TU)_4]^{2+}$ complex becomes the dominant species, shifting the ^{113}Cd NMR signal downfield. When compared to the ^{113}Cd NMR spectra of the methanol solutions **T4**−**T7** measured at room temperature (Figure 1, *right*), it is evident that the $[Cd(TU)_4]^{2+}$ complex dominates already at the mole ratio TU/Cd(II) = 4.0 in methanol, which is a much weaker ligand than water. We are unable to ascertain the degree of hydration m in the $[Cd(TU)_3(H_2O)_m]^{2+}$ complex, which is a minor species in solution according to the stability constants (Figure S-1), but we propose that the $[Cd(TU)_3(H_2O)_3]^{2+}$ complex is formed, as in the crystal structure.[52]

Comparison between Cd(II) Complex Formation with Selenourea and Thiourea in MeOH at ~200 K. The ^{113}Cd NMR spectra of 0.1 mol dm^{-3} $Cd(CF_3SO_3)_2$ solutions (Figure 1) in methanol containing 0.1−0.3 mol dm^{-3} selenourea (**S1**−**S3**) or thiourea (**T1**−**T3**) at 203 K show similar peaks in the 93−97 ppm and 189−194 ppm range, which were assigned to complexes with $Cd(Se/S)O_5$ and $Cd(Se/S)_2O_4$ coordination geometries, respectively. In this case the chemical shifts are very similar when one or two S/Se-donor ligands replace the O-donor ligands (methanol and $CF_3SO_3^-$ in the current case), in contrast to the generally observed trend with decreasing shielding of donor atoms in the following order: O ≫ Se > S.[43] Also, the formation constants for the CdL^{2+} and CdL_2^{2+} species are virtually the same for the SeU and TU systems, while $Cd(SeU)_3^{2+}$ and $Cd(SeU)_4^{2+}$ are more stable than the corresponding $Cd(TU)_3^{2+}$ and $Cd(TU)_4^{2+}$ complexes. The tris(thiourea)cadmium(II) complexes, $Cd(TU)_3^{2+}$, with CdS_3O_{1-3} coordination give rise to broad peaks at 333−337 ppm in the ^{113}Cd NMR spectra of the **T2**−**T3** solutions, while the tris(selenourea)cadmium(II) complexes with tetrahedral $CdSe_3O$ coordination correspond to the relatively sharp peak at 435 ppm, as for solutions **S1**−**S3**. In the methanol solutions **S4** and **S5**, containing 0.4−0.5 mol dm^{-3} selenourea, respectively, a $[Cd(SeU)_4]^{2+}$ complex with a $CdSe_4$ core is predominantly present. Its chemical shift $\delta(^{113}Cd)$ = 578 ppm is comparable to δ_{iso} = 577 ppm observed for CdS_4 coordination in the solid state ^{113}Cd NMR spectrum of $[Cd(TU)_4](NO_3)_2$ (Figure S-3) and is more deshielded than that of $[Cd(TU)_4]^{2+}$ (CdS_4, 526 ppm) in methanol solution at 203 K. Likewise, Isab and co-workers reported a more deshielded solid state ^{113}Cd NMR isotropic chemical shift for $Cd(SeU)_2Cl_2$ (458 ppm) than that for $Cd(TU)_2Cl_2$ (430 ppm).[36] The rather broad peak at 515 ppm for solution **T4**, containing 0.4 mol dm^{-3} thiourea, indicates that the $[Cd(TU)_4]^{2+}$ complex dominates; however, by increasing the ligand concentration, higher complexes with CdS_{5-6} coordination are formed.

CONCLUSION

In the current study, we have made a detailed evaluation of the speciation of cadmium(II) complexes with selenourea and thiourea by varying the ligand concentration, solvent, and temperature using a combination of spectroscopic methods, ^{113}Cd NMR, Cd K-edge EXAFS, and Cd L-edge XANES. In methanol solutions of 0.1 mol dm^{-3} $Cd(CF_3SO_3)_2$ with mole ratios L/Cd(II) ≤ 3.0 (L = SeU, TU), ^{113}Cd NMR spectroscopy shows mixtures of CdL_n^{2+} (n = 1−4) species in slow ligand exchange equilibria at 203 K, which allowed their stability constants to be estimated. In ligand excess, tetrahedral $[Cd(SeU)_4]^{2+}$ and $[Cd(TU)_4]^{2+}$ complexes dominate at 203 and 295 K, respectively, with the average bond distances Cd−Se 2.63 ± 0.02 Å and Cd−S 2.53 ± 0.02 Å, as determined by Cd K-edge EXAFS spectroscopy. When lowering the temperature from 295 to 203 K for 0.1 mol dm^{-3} $Cd(CF_3SO_3)_2$ methanol solutions with high mole ratios, TU/Cd(II) > 5.0, complexes with even higher thiourea coordination, $[Cd(TU)_{5-6}]^{2+}$, form to some extent.

In aqueous solutions of 0.1 mol dm^{-3} $Cd(CF_3SO_3)_2$ with increasing thiourea concentration, the ^{113}Cd NMR signal at 295 K corresponds to mixtures of $[Cd(TU)_y(H_2O)_{6-y}]^{2+}$ (y = 0−3) species in fast ligand exchange equilibria with $[Cd(TU)_4]^{2+}$ complexes. Higher excess of the thiourea ligand is needed than in comparable methanol solutions to form the $[Cd(TU)_4]^{2+}$ complex, which becomes the major species for free concentrations of thiourea exceeding ~0.4 mol dm^{-3}.

Based on the ^{113}Cd NMR chemical shifts observed in this study, Se (selone) and S (thione) donor atoms provide similar shielding effects in Cd(II) selenourea and thiourea complexes with similar coordination geometries. Almost identical $\delta(^{113}Cd)$ chemical shifts were observed at 203 K for the octahedrally coordinated $Cd(Se/S)O_5$ (δ ~ 95 ppm) and $Cd(Se/S)_2O_4$ species (δ ~ 190 ppm), with MeOH and possibly $CF_3SO_3^-$ as O-donor ligands. For the $[Cd(SeU)_4]^{2+}$ complex ($CdSe_4$ coordination), the chemical shift recorded at 578 ppm (MeOH, 203 K) is somewhat more deshielded than that of $[Cd(TU)_4]^{2+}$ (CdS_4 coordination, 526 ppm in MeOH at 203 K), although it is close to the isotropic chemical shift δ_{iso} (^{113}Cd) = 577 ppm for crystalline $[Cd(TU)_4](NO_3)_2$ measured at room temperature (Table 1).

When reporting ^{113}Cd NMR shifts, the coordination geometry is well-defined for crystalline Cd(II) complexes; however, in solution, the structure will not necessarily stay the same. Our method using X-ray absorption spectroscopy as a

dx.doi.org/10.1021/ic300852t | Inorg. Chem. 2012, 51, 10619−10630

supporting tool to further characterize the cadmium(II) species in solution significantly increases the insight in the systems studied. We have shown that ^{113}Cd NMR spectroscopy can be used for quite detailed speciation at LT in methanol solution, where for example the EXAFS technique was unable, on its own, to ascertain the partial formation of $[Cd(TU)_{5-6}]^{2+}$ complexes, as the overall increase in the Cd−S bond distances was ∼0.02 Å, within the error limit of EXAFS spectroscopy. Conversely, XAS spectroscopy was needed to structurally characterize the dominating species in the methanol solutions, especially to confirm that the Cd(II)−thiourea species with $\delta(^{113}Cd)$ = 526 ppm (541 ppm at 295 K) indeed is the $[Cd(TU)_4]^{2+}$ complex (CdS_4 coordination), which surprisingly has a more shielded chemical shift than $[Cd(SeU)_4]^{2+}$ with $\delta(^{113}Cd)$ = 578 ppm and $CdSe_4$ coordination.

We also show that thiourea, as a model for thione-containing ligands with neutral S-donor atoms, is more shielding than the thiolate groups with negatively charged S-donors, when comparing $[Cd(TU)_4]^{2+}$ with $\delta(^{113}Cd)$ = 541 ppm (in MeOH at 295 K) with the reported chemical shifts for Cd(II)-tetrathiolates (∼600−750 ppm). Therefore, caution should be exercised when interpreting sulfur coordination in biological systems based on ^{113}Cd NMR chemical shifts.

The individual chemical shifts obtained here are useful additions to the ^{113}Cd NMR chemical shifts previously reported for Cd(II)−thione complexes (Table 1), as well as cadmium(II) complexes with Se-donor ligands (Table 2). The ^{113}Cd NMR chemical shifts reported for cadmium(II) complexes with Se-donor ligands in general are altogether quite few,[88] as are also the crystal structures when compared with *S*-donor ligands, probably due to the air-sensitivity of most organo-selenium compounds.

■ ASSOCIATED CONTENT

Supporting Information

Total number of ^{113}Cd NMR scans collected for each sample and integrated peak areas for solutions **T1**−**T3** and **S1**−**S3**, solid state ^{113}Cd NMR spectra for crystalline $Cd(TU)_4(NO_3)_2$, $Cd(DMTF)_6(ClO_4)_2$, $Cd(DMTF)_4(CF_3SO_3)_2$, (HIm)[Cd(tsac)$_3$(H_2O)], and $[Cd(TU)_3(SO_4)]$, comparison between Cd K-edge EXAFS spectra of solutions **T4** and **T7** at LT/RT, comparison between the EXAFS spectra measured at 200 and 298 K for solutions **T1**, **T2**, and **T4**, EXAFS curve-fitting results for the aqueous Cd(II)−thiourea solutions **W1**−**W7**, a diagram showing the fractions of $Cd(TU)_x^{2+}$ (x = 0−4) species formed in aqueous solution vs total thiourea concentration, calculations regarding the average number of TU (/ SeU) per Cd(II) ion in solutions **S1**−**S3** and **T1**−**T3**, and fraction diagrams displaying the calculated distribution of $Cd(TU)_x$ and $Cd(SeU)_x$ (x = 0−4) species in methanol vs total TU or SeU concentration, respectively. This material is available free of charge via the Internet at http://pubs.acs.org.

■ AUTHOR INFORMATION

Corresponding Author

*E-mail: faridehj@ucalgary.ca.

Notes

The authors declare no competing financial interest.

■ ACKNOWLEDGMENTS

We are grateful to Qiao Wu, Dorothy Fox, and Jian Jun Li at the instrument facility at the Department of Chemistry, University of Calgary, for their skillful assistance in measuring the NMR spectra. Special thanks to Eun Young Kang for preparing the aqueous Cd(II) thiourea solutions (**W1**−**W7**). Beam time was allocated for X-ray absorption measurements at SSRL (Proposal No. 2848), which is operated by the Department of Energy, Office of Basic Energy Sciences, USA. The SSRL Biotechnology Program is supported by the National Institutes of Health, National Center for Research Resources, Biomedical Technology Program, and by the Department of Energy, Office of Biological and Environmental Research. We gratefully acknowledge the Natural Sciences and Engineering Council (NSERC) of Canada, Canadian Foundation for Innovation (CFI), Alberta Science and Research Investments Program (ASRIP), and the University of Calgary for providing financial support.

■ REFERENCES

(1) Erdelmeier, I.; Daunay, S.; Lebel, R.; Farescour, L.; Yadan, J.-C. *Green Chem.* **2012**, *14*, 2256−2265.
(2) Raper, E. S. *Coord. Chem. Rev.* **1985**, *61*, 115−184.
(3) Motohashi, N.; Mori, I.; Sugiura, Y. *Chem. Pharm. Bull.* **1976**, *24*, 1737−1741.
(4) Hanlon, D. P. *J. Med. Chem.* **1971**, *14*, 1084−1087.
(5) Motohashi, N.; Mori, I.; Sugiura, Y. *Chem. Pharm. Bull.* **1974**, *22*, 654 −657.
(6) Epand, R. M.; Epand, R. F.; Wong, S. C. *J. Clin. Chem. Clin. Biochem.* **1988**, *26*, 623 −626.
(7) Mayumi, T.; Okamoto, K.; Yoshida, K.; Kawai, Y.; Kawano, H.; Hama, T.; Tanaka, K. *Chem. Pharm. Bull.* **1982**, *30*, 2141−2146.
(8) Shannon, R. D. *Acta Crystallogr., A* **1976**, *A32*, 751−767.
(9) McMurray, C. T.; Tainer, J. A. *Nat. Genet.* **2003**, *34*, 239−241.
(10) Hartwig, A. *Antioxid. Redox Signal.* **2001**, *3*, 625−634.
(11) Allen, F. H. *Acta Crystallogr., B* **2002**, *B58*, 380−388.
(12) Ushasree, P. M.; Jayavel, R. *Opt. Mater.* **2003**, *21*, 599−604.
(13) Petrova, R.; Bakarjieva, S.; Todorov, T. *Z. Kristallogr.* **2000**, *215*, 118−121.
(14) Nardelli, M.; Gasparri, G. F.; Boldrini, P. *Acta Crystallogr.* **1965**, *18*, 618−623.
(15) Petrova, R.; Angelova, O.; Macícek, J. *Acta Crystallogr., C* **1997**, *53*, 565−568.
(16) Crow, D. R. *J. Chem. Soc., Faraday Trans. 1: Phys. Chem. Condensed Phases* **1986**, *82*, 3415−3430.
(17) Sankir, N. D.; Dogan, B. *J. Mater. Process. Technol.* **2011**, *211*, 382−387.
(18) Boev, V. I.; Soloviev, A.; Silva, C. J. R.; Gomes, M. J. M. *Solid State Sci.* **2006**, *8*, 50−58.
(19) Zou, L.; Fang, Z.; Gu, Z.; Zhong, X. *J. Lumin.* **2009**, *129*, 536−540.
(20) Chen, F.; Qiu, W.; Chen, X.; Yang, L.; Jiang, X.; Wang, M.; Chen, H. *Sol. Energy* **2011**, *85*, 2122−2129.
(21) O'Brien, P.; Saeed, T. *J. Cryst. Growth* **1996**, *158*, 497−504.
(22) Osterloh, F. E.; Hewitt, D. P. *Chem. Commun.* **2003**, 1700−1701.
(23) Moudgil, R.; Bharatam, P. V.; Kaur, R.; Kaur, D. *Proc.—Indian Acad. Sci., Chem. Sci.* **2002**, *114*, 223 −230.
(24) Chiesi, A.; Grossoni, G.; Nardelli, M.; Vidoni, M. E. *J. Chem. Soc., D: Chem. Commun.* **1969**, 404b−405.
(25) *Dangerous Prop. Ind. Mater. Rep.* **1995**, *15*, 105−113.
(26) Khlystunova, É. V.; Cheremisina, I. M.; Varand, V. L.; Shul'man, V. M. *Russ. Chem. Bull.* **1971**, *20*, 1448−1449.
(27) Markov, V.; Maskaeva, L. *Russ. J. Phys. Chem. A, Focus Chem.* **2010**, *84*, 1288−1293.
(28) Mel'checova, Z. E. *J. Appl. Chem. USSR* **1983**, *55*, 2471 −2475.
(29) Hendra, P. J.; Jovic, Z. *Spectrochim. Acta, Part A: Mol. Spectrosc.* **1968**, *24*, 1713−1720.
(30) Wazeer, M. I. M.; Isab, A. A.; Ahmad, S. *Can. J. Anal. Sci. Spectrosc.* **2006**, *51*, 43−48.

(31) Trujillo, C.; Mo, O.; Yanez, M.; Tortajada, J.; Salpin, J.-Y. *J. Phys. Chem. B* **2008**, *112*, 5479−5486.
(32) Hauge, S.; Tysseland, M. *Acta Chem. Scand. A* **1971**, *25*, 3072−3080.
(33) Jones, P. G.; Thöne, C. *Chem. Ber.* **1991**, *124*, 2725−2729.
(34) Henderson, W.; Nicholson, B. K.; Dinger, M. B. *Inorg. Chim. Acta* **2003**, *355*, 428−431.
(35) Aitken, G. B.; Duncan, J. L.; McQuillan, G. P. *J. Chem. Soc., Dalton Trans.* **1972**, 2103−2107.
(36) Isab, A. A.; Wazeer, M. I. M. *J. Coord. Chem.* **2005**, *58*, 529−537.
(37) Meteleva, Y.; Radychev, N.; Novikov, G. *Inorg. Mater.* **2007**, *43*, 455−465.
(38) Epifani, M.; Giannini, C.; Manna, L. *Mater. Lett.* **2004**, *58*, 2429−2432.
(39) Feroci, G.; Badiello, R.; Fini, A. *J. Trace Elem. Med. Biol.* **2005**, *18*, 227−234.
(40) Golovnev, N.; Leshok, A.; Novikova, G.; Petrov, A. *Russ. J. Inorg. Chem.* **2010**, *55*, 130−132.
(41) Goddard, D. R.; Lodam, B. D.; Ajayi, S. O.; Campbell, M. J. *J. Chem. Soc. A: Inorg., Phys., Theor.* **1969**, 506−512.
(42) Ellis, P. D. *Science* **1983**, *221*, 1141−1146.
(43) Summers, M. F. *Coord. Chem. Rev.* **1988**, *86*, 43−134.
(44) Eichele, K.; Wasylishen, R. E. *Inorg. Chem.* **1994**, *33*, 2766−2773.
(45) Öz, G.; Pountney, D. L.; Armitage, I. M. *Biochem. Cell Biol.* **1998**, *76*, 223−234.
(46) Rajalingam, U.; Dean, P. A. W.; Jenkins, H. A.; Jennings, M.; Hook, J. M. *Can. J. Chem.* **2001**, *79*, 1330−1337.
(47) Craig, D. C.; Dance, I. G.; Dean, P. A. W.; Hook, J. M.; Jenkins, H. A.; Kirby, C. W.; Scudder, M. L.; Rajalingam, U. *Can. J. Chem.* **2005**, *83*, 174−184.
(48) Stålhandske, C. M. V.; Stålhandske, C. I.; Sandstrom, M.; Persson, I. *Inorg. Chem.* **1997**, *36*, 3167−3173.
(49) Tarulli, S. H.; Quinzani, O. V.; Baran, E. J.; Piro, O. E.; Castellano, E. E. *J. Mol. Struct.* **2003**, *656*, 161−168.
(50) Oussaïd, M.; Becker, P.; Carabatos-Nédelec, C. *J. Raman Spectrosc.* **2000**, *31*, 529−533.
(51) Amo-Ochoa, P.; Rodíguez-Tapiador, M. I.; Castillo, O.; Olea, D.; Guijarro, A.; Alexandre, S. S.; Gómez-Herrero, J.; Zamora, F. *Inorg. Chem.* **2006**, *45*, 7642−7650.
(52) Parvez, M.; Jalilehvand, F.; Amini, Z. *Acta Crystallogr., E* **2012**, *68*, m949−m950.
(53) Lee, G. S. H.; Fisher, K. J.; Vassallo, A. M.; Hanna, J. V.; Dance, I. G. *Inorg. Chem.* **1993**, *32*, 66−72.
(54) Mennitt, P. G.; Shatlock, M. P.; Bartuska, V. J.; Maciel, G. E. *J. Phys. Chem.* **1981**, *85*, 2087−2091.
(55) Bond, A. M.; Colton, R.; Ebner, J.; Ellis, S. R. *Inorg. Chem.* **1989**, *28*, 4509−4516.
(56) Demko, B. A.; Wasylishen, R. E. *Dalton Trans.* **2008**, 481−490.
(57) Yu, K.; Ouyang, J.; Zaman, M. B.; Johnston, D.; Yan, F. J.; Li, G.; Ratcliffe, C. I.; Leek, D. M.; Wu, X.; Stupak, J.; Jakubek, Z.; Whitfield, D. *J. Phys. Chem. C* **2009**, *113*, 3390−3401.
(58) Mikulec, F. V.; Kuno, M.; Bennati, M.; Hall, D. A.; Griffin, R. G.; Bawendi, M. G. *J. Am. Chem. Soc.* **2000**, *122*, 2532−2540.
(59) Carson, G. K.; Dean, P. A. W. *Inorg. Chim. Acta* **1982**, *66*, 37−39.
(60) Wazeer, M. I. M.; Isab, A. A. *Spectrochim. Acta, Part A: Mol. Biomol. Spectrosc.* **2005**, *62*, 880−885.
(61) Subramanian, R.; Govindaswamy, N.; Santos, R. A.; Koch, S. A.; Harbison, G. S. *Inorg. Chem.* **1998**, *37*, 4929−4933.
(62) Kedarnath, G.; Kumbhare, L. B.; Jain, V. K.; Phadnis, P. P.; Nethaji, M. *Dalton Trans.* **2006**, 2714−2718.
(63) Sharma, R. K.; Kedarnath, G.; Wadawale, A.; Jain, V. K.; Vishwanadh, B. *Inorg. Chim. Acta* **2011**, *365*, 333−339.
(64) Ng, M. T.; Dean, P. A. W.; Vittal, J. J. *Dalton Trans.* **2004**, 2890−2894.
(65) Godovsky, D. Y.; Varfolomeev, A. E.; Zaretsky, D. F.; Nayana Chandrakanthi, R. L.; Kundig, A.; Weder, C.; Caseri, W. *J. Mater. Chem.* **2001**, *11*, 2465−2469.
(66) Ammann, C.; Meier, P.; Merbach, A. *J. Magn. Reson.* **1982**, *46*, 319−321.
(67) George, G. N.; George, S. J.; Pickering, I. J. EXAFSPAK. Menlo Park, CA, Stanford Synchrotron Radiation Lightsource (SSRL). 2001.
(68) Ressler, T. *J. Synchrotron Radiat.* **1998**, *5*, 118−122.
(69) Jalilehvand, F.; Leung, B. O.; Mah, V. *Inorg. Chem.* **2009**, *48*, 5758−5771.
(70) Zabinsky, S. I.; Rehr, J. J.; Ankudinov, A.; Albers, R. C.; Eller, M. J. *Phys. Rev. B* **1995**, *52*, 2995−3009.
(71) Ankudinov, A. L.; Rehr, J. J. *Phys. Rev. B* **1997**, *56*, R1712 − R1716.
(72) Ravel, B. *J. Synchrotron Radiat.* **2001**, *8*, 314−316.
(73) Bharara, M. S.; Kim, C. H.; Parkin, S.; Atwood, D. A. *Polyhedron* **2005**, *24*, 865−871.
(74) Williams, D.; McKinney, B.; Baker, B.; Gwaltney, K.; VanDerveer, D. *J. Chem. Crystallogr.* **2007**, *37*, 691−694.
(75) Zhang, Y.; Li, J.; Chen, J.; Su, Q.; Deng, W.; Nishiura, M.; Imamoto, T.; Wu, X.; Wang, Q. *Inorg. Chem.* **2000**, *39*, 2330−2336.
(76) Jalilehvand, F.; Leung, B. O.; Izadifard, M.; Damian, E. *Inorg. Chem.* **2006**, *45*, 66−73.
(77) Pickering, I. J.; Prince, R. C.; George, G. N.; Rauser, W. E.; Wickramasinghe, W. A.; Watson, A. A.; Dameron, C. T.; Dance, I. G.; Fairlie, D. P.; Salt, D. E. *Biochim. Biophys. Acta* **1999**, *1429*, 351−364.
(78) Isaure, M.-P.; Fayard, B.; Sarret, G.; Pairis, S.; Bourguignon, J. *Spectrochim. Acta, B* **2006**, *61*, 1242−1252.
(79) Jalilehvand, F.; Mah, V.; Leung, B. O.; Mink, J.; Bernard, G. M.; Hajba, L. *Inorg. Chem.* **2009**, *48*, 4219−4230.
(80) Honkonen, R. S.; Marchetti, P. S.; Ellis, P. D. *J. Am. Chem. Soc.* **1986**, *108*, 912−915.
(81) Ueyama, N.; Sugawara, T.; Sasaki, K.; Nakamura, A.; Yamashita, S.; Wakatsuki, Y.; Yamazaki, H.; Yasuoka, N. *Inorg. Chem.* **1988**, *27*, 741−747.
(82) Udupa, M. R. *J. Indian Chem. Soc.* **1972**, *49*, 775.
(83) Bensch, W.; Schuster, M. *Z. Anorg. Allg. Chem.* **1993**, *619*, 791−795.
(84) Liu, C. W.; Chen, J.-M.; Santra, B. K.; Wen, S.-Y.; Liaw, B.-J.; Wang, J.-C. *Inorg. Chem.* **2006**, *45*, 8820−8822.
(85) Lacelle, S.; Stevens, W. C.; Kurtz, D. M.; Richardson, J. W.; Jacobson, R. A. *Inorg. Chem.* **1984**, *23*, 930−935.
(86) Dolega, A.; Baranowska, K.; Gajda, J.; Kazmierski, S.; Potrzebowski, M. J. *Inorg. Chim. Acta* **2007**, *360*, 2973−2982.
(87) Murphy, P. D.; Stevens, W. C.; Cheung, T. T. P.; Lacelle, S.; Gerstein, B. C.; Kurtz, D. M. *J. Am. Chem. Soc.* **1981**, *103*, 4400−4405.
(88) Rajalingam, U.; Dean, P. A. W.; Jenkins, H. A. *Can. J. Chem.* **2000**, *78*, 590−597.